


Characterization of the Expression of Vacuolar Protein Sorting II (VpsII) in Mammalian Oligodendrocytes

ASN Neuro
Volume 13: 1–17
© The Author(s) 2021
Article reuse guidelines:
sagepub.com/journals-permissions
DOI: 10.1177/17590914211009851
journals.sagepub.com/home/asn


Robert P. Skoff, Denise Bessert, Shreya Banerjee, Xixia Luo, and Ryan Thummel 

Abstract

A founder mutation in human *VPS11* (*Vacuolar Protein Sorting II*) was recently linked to a genetic leukoencephalopathy in Ashkenazi Jews that presents with the classical features of white matter disorders of the central nervous system (CNS). The neurological deficits include hypomyelination, hypotonia, gradual loss of vision, and seizures. However, the cells expressing the mutation were not identified. Here we describe, using immunocytochemistry, the strong expression of VpsII in mouse oligodendrocytes and, specifically, its localization with Myelin Associated Glycoprotein (MAG) in the inner tongue of myelin. In longitudinal sections of myelin, it forms a bead-like structure, alternating with Myelin Basic Protein (MBP). Immunofluorescent staining with VpsII and neurofilament proteins indicates the absence of VpsII in axons *in vivo*. Finally, changes in VpsII expression are associated with altered proteolipid protein (PLP) levels based upon mice with duplications or deletions of the *Plp1* gene. To determine potential functional contributions of VpsII, we combined VpsII with Platelet Derived Growth Factor Receptor- α (PDGFR α) *in vitro* and *in vivo*: in both conditions, co-localization of the two proteins was frequently found in round vesicles of OPCs/oligodendrocytes, suggesting retrograde transport for degradation by the endolysosomal system. Neuron-to-glia communication has been invoked to explain degenerative changes in myelin followed by degenerative changes in axons, and vice versa; but to our knowledge, no specific proteins in retrograde transport from the myelin inner tongue to oligodendrocyte perikarya have been identified. The identification of mutations in *VPS11* and its localization at the axon-myelin interface should open new avenues of research.

Keywords

myelination, neurodevelopmental disorders, lysosomal storage diseases, neurodegenerative diseases, genetic neurodevelopmental and neurodegenerative disorders, oligodendrocytes

Received June 30, 2020; Revised March 18, 2021; Accepted for publication March 20, 2021

Introduction

Vacuolar protein sorting (Vps) proteins play an evolutionarily conserved role in the transport of molecules within the endolysosomal system. Endocytic vesicles arising from the plasma membrane fuse with early endosomes via the function of the tethering proteins EEA1, Rabenosyn-5, and Vac1 (Christoforidis et al., 1999; Tall et al., 1999; Nielsen et al., 2000). Following fusion with early endosomes, Vps proteins function as part of a cluster of proteins that aid in homotypic fusion of the endocytic organelles. More specifically, a group of four Vps proteins (Vps11, Vps16, Vps18, and Vps33) serve as the protein core for two tethering complexes, the class C core vacuole/endosome tethering complex (CORVET) and the

homotypic fusion and protein sorting complex (HOPS) (Balderhaar and Ungermann, 2013; Takemoto et al., 2018). CORVET coordinates binding and functions

Department of Ophthalmology, Visual and Anatomical Sciences, Wayne State University School of Medicine, Detroit, Michigan, United States.

Corresponding Authors:

Robert P. Skoff, Department of Ophthalmology, Visual and Anatomical Sciences, Wayne State University School of Medicine, Detroit, Michigan, United States.

Email: rskoff@med.wayne.edu

Ryan Thummel, Department of Ophthalmology, Visual and Anatomical Sciences, Wayne State University School of Medicine, Detroit, Michigan, United States.

Email: rthummel@med.wayne.edu



with a GTPase bound to early endosomes, Rab5, to assist in homotypic endosome-endosome fusion (Markgraf et al., 2009). Rab7 replaces Rab5 on late endosomes/lysosomes and coordinates with the HOPS complex in late endosome-lysosome fusion and autophagosome-lysosome fusion (Peplowska et al., 2007; van der Kant et al., 2015). The majority of our understanding of the function of Vps proteins is based on their identification and well-established function in yeast (Banta et al., 1988; Raymond et al., 1992). Mammalian homologs of the CORVET and HOPS complexes have been confirmed to function in early endosome fusion, late endosome-lysosome fusion, and autophagosome-lysosome fusion (Jiang et al., 2014; Perini et al., 2014; McEwan et al., 2015; Wartosch et al., 2015). However, compared to work done in yeast, our understanding of their structure and function in mammals is limited, especially in regard to their function in the mammalian central nervous system (CNS) (Nickerson et al., 2009; Balderhaar and Ungermann, 2013; Spang, 2016).

Recently, a founder missense mutation in human *VPS11* (C2536T>G(p.C846G)) was linked to a genetic leukoencephalopathy in Ashkenazi Jews, manifesting as classical features of white matter disorders of the CNS (Zhang et al., 2016). These included hypomyelination, motor disability, hypotonia, gradual loss of vision, and seizures amongst other neurological disorders (Edvardson et al., 2015; Zhang et al., 2016). The *VPS11* mutation leads to aberrant ubiquitination and reduced VPS11 expression as well as reduced interaction with its neighboring protein, VPS18 (Zhang et al., 2016). Theoretically, the HOPS and CORVET complexes are ubiquitously expressed in all cells, and therefore all cells of the CNS of individuals who carry the *VPS11*: C2536T>G(p.C846G) mutation are likely affected. A recent single-cell RNAseq analysis found a relative equal distribution of *Vps11* mRNA within cells from the mouse cortex (Zeisel et al., 2015). However, based upon the neurological findings and hypomyelination in these patients, oligodendrocytes are a likely target of the mutation.

We conducted Vps11 immunocytochemical analysis of normal mouse brains with antibodies to Vps11, oligodendrocytes, myelin proteins, and axonal markers. Intriguingly, we found *in vivo* and *in vitro* that Vps11 is strongly expressed in developing and mature oligodendrocytes. In low magnification profiles of immunocytochemically-stained brains, Vps11 appears to be co-localized to compact myelin, but at higher magnification, it does not co-localize with compact myelin. Instead, we found that Vps11 is expressed around the inner and outer cytoplasmic loops of myelin. Based upon combined Vps11 and neurofilament staining, Vps11 is not present in the axon, but there is modest co-localization of Vps11 and Myelin Associated Glycoprotein (MAG) in the inner cytoplasmic loop of the oligodendrocyte. Interestingly, changes in Vps11 expression are associated

with mutations of myelin proteolipid protein (PLP); Vps11 expression is higher in *Plp1* null mice and lower in transgenic mice with *Plp1* duplications.

This publication is the first to describe the unique distribution of Vps11 within the mammalian CNS. Its strong expression in oligodendrocytes, its location to the inner tongue of myelin, and its co-localization with Platelet Derived Growth Factor Receptor- α (PDGFR α) and lysosomes raises the possibility that it is involved in endosomal recycling and transport of molecules from the axon-myelin interface back to the oligodendrocyte cell body for lysosomal degradation.

Materials and Methods

Animals

Four strains of mice were used for these studies: wild-type C57BL/6J and B6129SF1/J (Jackson Laboratory, Bar Harbor, ME), *Plp1* null mutant mice (Klugmann et al., 1997), and *Plp1* mice with duplications of the *Plp1* gene (Readhead et al., 1994). Genotyping was confirmed by standard genotyping of tail clips as previously reported (Appikarla et al., 2014). All mice were housed in the Department of Laboratory Animals Resources (DLAR) animal facilities at Wayne State University, a federally approved AAALAC facility under direct supervision of DLAR staff. All procedures were approved by the local Institutional Animal Care and Use Committee (IACUC) committee.

Immunocytochemistry of Brains

Following terminal anesthesia, mice were intracardially perfused with 4% paraformaldehyde in 0.1 M phosphate buffered saline (PBS); brains were removed and stored in 4% paraformaldehyde at 4°C. Fifty-micron transverse sections of brains were cut on a Vibratome (Ted Pella, Redding CA) and stored in PBS prior to processing for immunocytochemistry.

Horseradish Peroxidase Immunodetection of Vps11. Brain sections were washed in PBS with 2% TritonX-100 (prod. no. X-100, Sigma-Aldrich USA, St. Louis, MO) for 1 hr at room temperature (RT). Sections were additionally washed several times in PBS, treated with 3% hydrogen peroxide for 20 min at RT, washed again in PBS, and then incubated in 10% donkey serum (prod. no. 017-000-121, Jackson ImmunoResearch, West Grove, PA) in PBS for 1 hr at RT. Sections were then placed in goat polyclonal anti-VPS11 (prod. no. ab-40816, 1:100; Abcam; Cambridge, MA) in PBS overnight at RT. The following day, sections were incubated in horseradish peroxidase conjugated anti-goat (prod. no. 705-035-003, Jackson ImmunoResearch) 1:100 in PBS for 2 hrs at RT and then washed in PBS. To detect

specific staining, sections were then incubated in 3,3'-Diaminobenzidine (DAB) substrate SigmaFast (prod. no. D4293, Sigma-Aldrich), washed in PBS, and mounted on glass slides with Aqua-Poly/Mount (prod. no. 18606, Polysciences, Inc., Warrington, PA). Sections lacking primary antibody incubation were used as controls. Sections were imaged on a Leitz Laborlux 12 microscope using a SPOT Flex camera and software. Selected images from wild-type mice, *Plp1* null mice, and *Plp1* mice with duplications were inverted in Adobe Photoshop and histograms of the areas of interest were measured using Image J. Averages were calculated and graphed using Excel, and statistical differences between the groups were determined by a one-way ANOVA with a post-hoc Tukey test.

Immunofluorescence of Vps11, Oligodendrocytes, and Myelin Proteins *in vivo*. Sections were processed as described above and then incubated with primary antibodies using antigen retrieval protocols as previously described (Appikatta et al., 2014). Briefly, following a wash in 0.1 M PBS, sections were incubated in an antigen retrieval solution (10 mM citrate buffer pH6.0 and 0.1% Tween20 (prod. no. P5927, Sigma-Aldrich) for 20 min at 80 °C, followed by 40 min at RT. Next, sections were washed in PBS and incubated in primary antibody solution overnight at RT. The following primary antibodies were utilized: goat polyclonal anti-Vps11 (prod. no. ab-40816, 1:100; Abcam), mouse monoclonal anti-Myelin Basic Protein (MBP, prod. no. 836504 1:1000, clone SMI 94; BioLegend; San Diego, CA), mouse monoclonal anti-Neurofilament-L (NF-L) (prod. no.2835, 1:100; Cell Signaling; Danvers, MA), mouse monoclonal anti-Neurofilament 200 (NF200, prod. no. N-0142, 1:100; Sigma-Aldrich; St. Louis, MO), and rabbit polyclonal anti-Myelin-associated glycoprotein (MAG, 1:1000, gift from Richard Quarles, Bethesda, DC) (Sternberger et al., 1979).

For double immunofluorescence with Vps11 and MBP, sections were treated with 2% Triton X-100 for 1 hr, washed in PBS, then incubated in polyclonal anti-Vps11 and monoclonal anti-MBP primary antisera overnight at RT. The following day sections were washed in PBS and then incubated in anti-goat Alexa 594 (prod. no. A-21468, 1:400; Invitrogen) and anti-mouse Alexa 488 (prod. no. A-21200, 1:400; Invitrogen) for 2 hrs at RT. For double immunofluorescence with Vps11 and either MAG, NF-L or NF200, sequential immunolabeling was performed. Briefly, sections were incubated overnight in either anti-MAG, anti-NF-L, or anti-NF200, washed in PBS, incubated in the corresponding secondary antibody, anti-rabbit Alexa 488 (prod.no. 111-545-144, Jackson ImmunoResearch) for MAG or anti-mouse Alexa 488 (prod. no. 115-545-146, Jackson ImmunoResearch) for NF-L and NF200 for 2 hrs at RT, and then washed in PBS. Next, the sections were incubated overnight in anti-Vps11 at RT, washed in PBS, then incubated in anti-goat

Alexa 594 (1:400) for 2 hrs at RT. Finally, the sections were incubated with DAPI (prod. no. 10236276001, 1:10,000; Roche; Indianapolis, IN) in methanol for 5 min, washed again in PBS, and then mounted on glass slides with Aqua-Poly/Mount. Confocal images were obtained using a Leica SP5 confocal microscope. Selected images noted in the text were deconvolved using Huygens Deconvolution (Scientific Volume Imaging, Laapersveld, Netherlands). Images were imported into Adobe Photoshop to create figures.

Western Blot Analysis

Protein was extracted from mouse brain hemispheres by homogenizing the tissue in lysis buffer containing protease inhibitor cocktail (Pierce Protease Inhibitor mini tablets, prod.no. 88666, ThermoScientific). Three separate mouse brains were used per genotype (n = 9 total hemispheres). Total protein concentration was determined with Quick Start Bradford protein assay (prod. no. 500-0201, Bio-Rad). 15 µg of total protein isolated per sample was separated using 8% SDS-PAGE under reducing conditions, followed by electrophoretic transfer onto polyvinylidene difluoride (PVDF) membranes (GE healthcare Life Science, Fisher Scientific). The membranes were blocked with Blotting-grade Blocker (prod. no. 170-6404, Bio-Rad) for 1 hr at RT followed by incubation with rabbit monoclonal anti-VPS11 antibody (prod. no. ab189920, 1:500, Abcam) overnight at 4 °C. The following day, blots were incubated in anti-rabbit IgG horseradish peroxidase antibody (prod. no. 31460, 1:5,000, ThermoScientific) for 2 hrs at RT. The bands were detected using Western Lighting Plus-ECL chemiluminescence (prod. no. NEL103E001EA, PerkinElmer) and imaged with FluorChem System (ProteinSimple). For the loading control, mouse monoclonal IgG β-Actin (C4) HRP (Santa Cruz Biotechnology, prod. No. sc-47778 HRP, 1:2500) was applied to the membrane and incubated overnight at 4 °C, followed by detection and imaging as described above. The intensity density of each band was analyzed by ImageJ and the Vps11 signal was normalized to the intensity of the corresponding β-Actin control. A one-way ANOVA was performed to determine statistical differences between all three genotypes and a post-hoc Tukey test was used to determine statistical differences between each genotype. The graphical representation of the data was presented as changes in normalized Vps11 expression relative to wild-type control samples.

Immunocytochemistry of Oligodendrocyte Cultures

Primary glial cultures were prepared via routine lab procedures (Knapp et al., 1987) from male and female mouse brains that were separately grown in 100 mm Petri dishes

(2 brains/dish) coated with 100 µg/ml polylysine (prod. no. P1399; Sigma-Aldrich). They were grown in DMEM media (prod. no. 11,965; Thermo Fisher Scientific) containing 10% FBS (prod. no. A1115-N, Hyclone; Thermo Fisher Scientific) and 1% antibiotic and antimycotic drugs (prod. no. 15240062; Gibco, Thermo Fisher Scientific) for 9–10 days, at which time the cells became confluent. Then, the upper layer of cells containing mostly oligodendrocyte precursors and oligodendrocytes was dislodged by gently blowing the cells with media using a 10-cc syringe attached to a 21-gauge needle. The cells were collected with the media and plated onto another uncoated 100 mm Petri dish, to allow microglia and astrocytes to adhere to the dish. After 30 minutes, floating cells, which are mostly oligodendrocyte precursors and oligodendrocytes, were collected with a 5-cc pipette, transferred into a 15-cc centrifuge tube, spun down, and counted using a hemocytometer; then, an equal number of cells (about 7,000 cells/coverslip) from male and female oligodendrocytes were plated onto 20 µg/ml polylysine coated 12 mm coverslips. From one Petri dish, we obtain enough oligodendrocyte progenitors/oligodendrocytes for 24 coverslips. Secondary cultures were grown for 4–5 days prior to immunostaining. For immunohistochemistry, coverslips with oligodendrocytes were washed with PBS, fixed with cold 4% paraformaldehyde for 10 min, washed in PBS, incubated in an antigen retrieval solution as described previously for 15 min at 80 °C, followed by 30 min at RT, washed in PBS and incubated in primary antibody for one hour at RT. The following primary antibodies were utilized: goat polyclonal anti-Vps11 (1:100, Abcam), rat monoclonal AA3 anti-PLP (1:50, gift of Marjorie Lees), mouse monoclonal IgG1 anti-GFAP (Glial Fibrillary Acidic Protein; prod. no. 3670S, 1:100; Cell Signaling, Danvers MA), rat monoclonal anti-Lamp2 (Lysosome-associated Membrane Protein 2; prod. no. sc-20004, 1:100; Santa Cruz, Dallas TX), rabbit monoclonal anti-PDGFR α (prod. no. 3174S, 1:100; Cell Signaling, Danvers MA), and rabbit anti-EEA1 (Early Endosomal Antigen 1; prod. No. 3288, 1:100; Cell Signaling, Danvers MA). Following incubation in primary antibody, cells were washed in PBS and incubated in anti-primaries conjugated to either Alexa 488 or 594 (1:400) for 2 hrs at RT, washed in PBS, incubated in DAPI (1:10,000 in methanol) for 5 mins, washed in PBS, and mounted onto slides with Aqua-Poly/Mount. For Vps11 and PLP immunostaining, Vps11 was the first primary followed by anti-goat Alexa 594 as the secondary and then the primary antibody for PLP was added followed by its appropriate secondary. For all other double immunocytochemistry, Vps11 with either GFAP, PDGFR α , Lamp2 or EEA1, the procedure was performed by incubating in both primary antibodies

simultaneously and followed by both secondary incubations simultaneously.

Results

Vps11 Is Strongly Expressed in Oligodendrocytes and Is Closely Associated With Compact Myelin

In enriched oligodendrocyte cultures prepared from 3-day postnatal (DPN) mouse brains, Vps11 expression was localized to the perikarya and processes of immature oligodendrocytes (OPCs) (Figure 1A to C). As OPCs differentiated into oligodendrocytes, both PLP and Vps11 were expressed in the veins of their membranous sheets (Figure 1D to F, arrows in F). Small, unidentified DAPI-labeled cells were not Vps11 immunolabeled (Figure 1F, asterisks). However, cells with flattened, sheet-like cytoplasm and/or straight and thick processes, were Vps11 and GFAP positive (Figure 1G to I). Similar to *in vitro* expression of Vps11, oligodendrocytes in Vibratome-sectioned mouse brains at 15DPN were immuno-positive for Vps11 (Figure 1J to L). Vps11-immunostained cells had the characteristic morphology of oligodendrocytes in the corpus callosum and striatum (Figure 1J to K, arrow), with round or oval shapes of myelinating oligodendrocytes, and they often showed thin processes connected to myelin. Transverse sections of myelinated axons from the basal ganglia showed a double band of Vps11 immunostaining surrounding compact myelin (Figure 1L, arrows). In contrast to the *in vitro* results, we did not observe strong staining of other cell types, including neurons, microglia, and astrocytes, identified by their size and shape (Figures 1 and 2). Finally, elimination of primary Vps11 antibody from immunocytochemical staining showed no positive staining (Figure 1J, inset).

In co-localization studies of 15DPN mouse brains, Vps11 and MBP expression was observed in the oligodendrocyte cell soma (Figure 2A to F). For the most part, Vps11 and MBP were not co-localized to the same cytoplasmic compartments; however, there was some overlap (Figure 2A to F). This observation was predicted given that MBP is translated on free ribosomes (Muller et al., 2013). We were unable to find both strong MBP and Vps11 immunostaining in the perikarya of 30DPN and older animals (data not shown). This result was in keeping with previous findings that detection of MBP in oligodendrocyte cytoplasm *in vivo* is best observed in young oligodendrocytes (Sternberger et al., 1978). However, Vps11 and MBP co-localization was readily observed in/near myelin sheaths *in vivo* at multiple ages (Figure 2G to L). In longitudinal sections of fibers, MBP was found along the length of the fiber, sometimes co-localized with Vps11 but for the most part the two were observed in separate compartments (Figure 2G to L). See Discussion for interpretation of

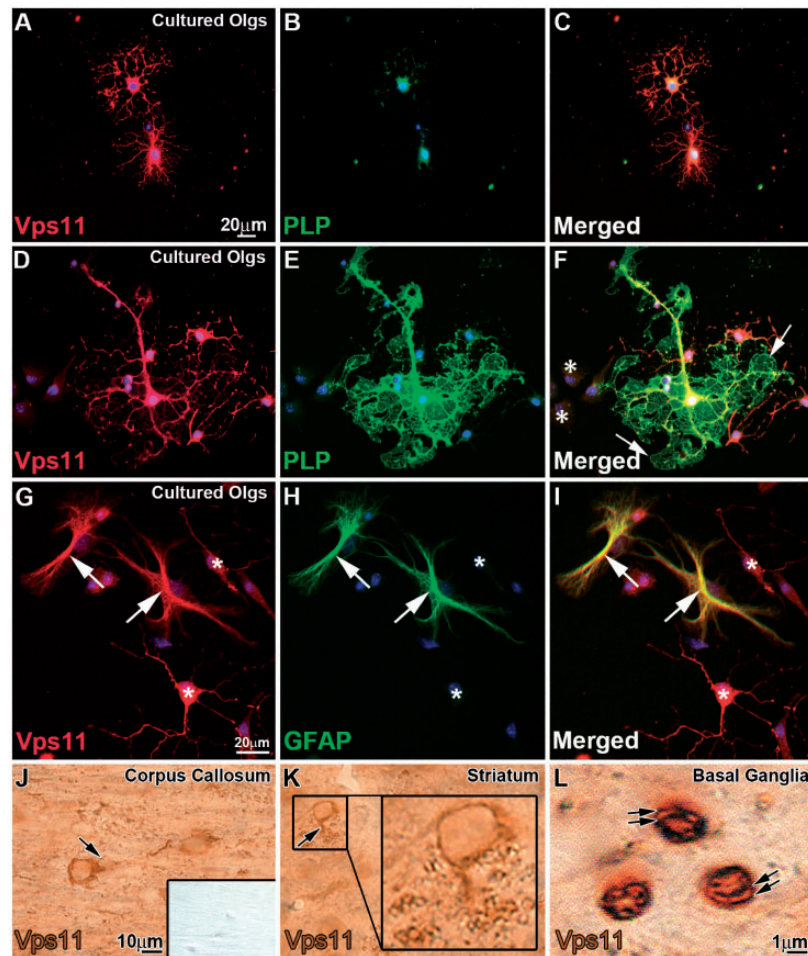


Figure 1. Vps11 Is Strongly Expressed in Oligodendrocytes. A to F: Oligodendrocyte (Olg) cultures prepared from 3DPN mouse brain labeled with PLP (green), Vps11 (red), and DAPI (blue). D to F: A mature Olg, identified by large membranous sheets, stains with both PLP (green) and Vps11 (red) that are abundant throughout the veins of the Olg. F: PLP (green, arrows) stains the plasma membrane in several areas lacking Vps11. Several immature Olg are also stained for Vps11 (red only). G to I: In tissue culture, astrocytes (arrows) stain for Vps11 (red) as well as immature Olg (asterisks) which are negative for GFAP. J to L: Fifty-micron Vibratome brain sections from the Corpus Callosum, Striatum, and Basal Ganglia of a 15DPN mouse immunostained with Vps11 and developed with DAB. Sections lacking primary antibody as control (inset for J) exhibited no staining. J to K: The round, cellular profiles and smooth, spherically stained nuclei are characteristic of Olg. Processes of these cells (arrows) extend into neuropil where they presumably myelinate axons. L: High-magnification transverse sections of myelinated axons suggesting that Vps11 is highly expressed in the inner (abaxonal) and outer (periaxonal) loops (arrows).

“co-localized” antibodies. Vps11 clearly localized to numerous bead-like structures interspersed between MBP along the myelin sheath (Figure 2L, arrows), suggestive of its localization to cytoplasmic compartments and/or longitudinal incisures.

Co-immunostaining of Vps11 and myelin associated glycoprotein (MAG) revealed a unique localization of Vps11 to the inner cytoplasmic tongue of myelin (Figure 3). In transverse sections of the same fiber, the Vps11-positive process of an oligodendrocyte that initially extended outside the MAG-positive inner tongue (Figure 3A and B); however, as confocal images were

captured deeper through the z-plane of the fiber, the two proteins clearly localized to the same compartment (Figure 3G and H). In the MAG-positive inner tongue, the expression of the two proteins overlapped nearly completely. Co-immunostaining of Vps11 and MBP in transverse sections of fibers confirmed that Vps11 stains both inner and outer myelin but is negligible in compact myelin (Figure 3I to P), suggestive of its localization to both the outer (abaxonal) and inner (periaxonal) compartments (Figure 3Q to R). Collectively, these data provide evidence that the endolysosomal system involving the C-Vps proteins extends to the compartment

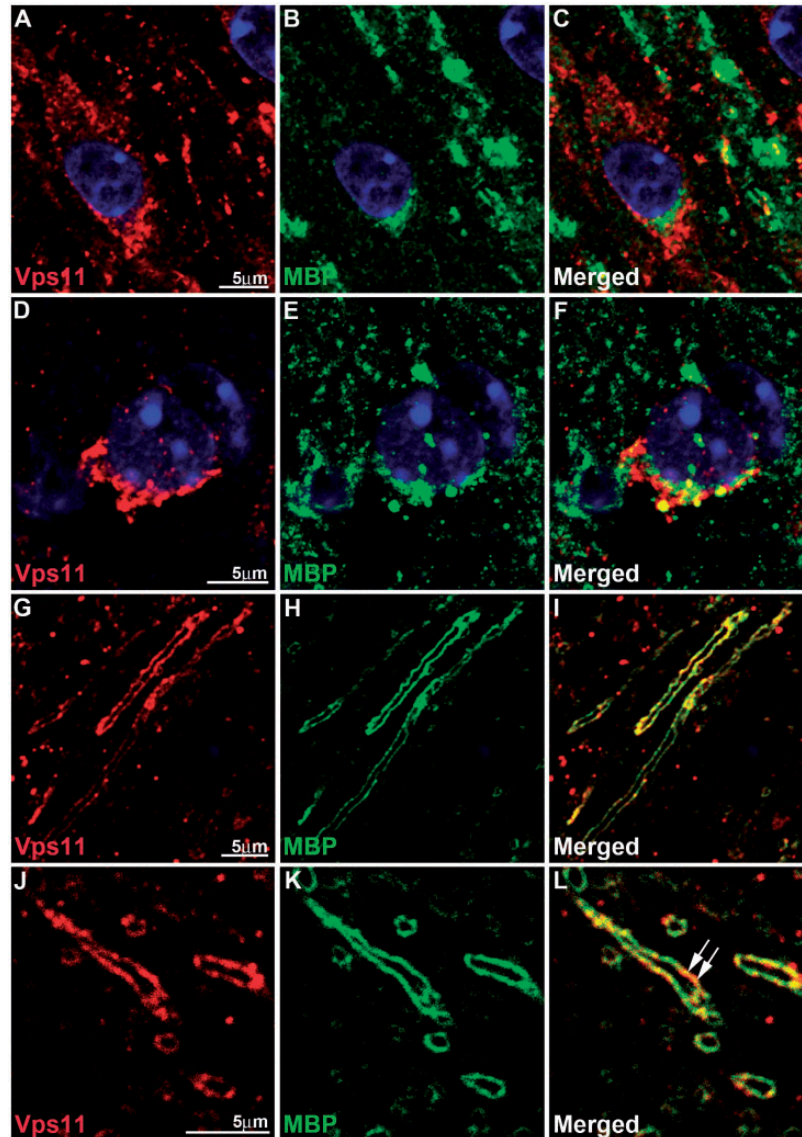


Figure 2. Vps11 Is Strongly Expressed in Oligodendrocytes in Vivo. A to F: Confocal images from the ventral Basal Ganglia of a 15DPN mouse co-immunostained with MBP (green) and Vps11 (red) antibodies. Vps11 and MBP expression in the oligodendrocyte cell soma are generally in separate cytoplasmic compartments but co-localization (yellow) (F) is also found in some cells. G to L: Confocal images from the cerebrum of a 15DPN mouse co-immunostained with MBP (green) and Vps11 antibodies (red). Vps11 localizes to numerous bead-like structures (arrows, L) in longitudinal and transverse cuts throughout the myelin sheath but separate from MBP in compact myelin.

immediately adjacent to the axon, and suggest a model of a functional role for C-Vps proteins in oligodendrocyte/neuron cross-talk (Figure 3Q to R).

Vps11 Expression Is Altered in Plp1 Null Mutants and Plp1 Overexpression Mice

To test whether expression of C-Vps proteins are altered in different metabolic states, we analyzed Vps11 expression in *Plp1* null mutant mice (Klugmann et al., 1997) and *Plp1* mice with duplications (Readhead et al., 1994). At low magnification, Vps11 immunolabeled fiber tracks

that mimic the immunostaining observed with various myelin antibodies (Figure 4A). However, as shown in Figures 1 to 3, Vps11 did not co-localize within compact myelin. Interestingly, Vps11 immunostaining was significantly increased in the corpus callosum, the cerebral cortex immediately above the corpus callosum, and the basal ganglia of 30DPN *Plp1* null mice when compared with expression in wild-type siblings (Figures 4 and 5; $p < 0.01$). In contrast, Vps11 immunostaining was significantly decreased in *Plp1* mice with duplications (Figures 4 and 5; $p < 0.01$). Higher magnification of these 3 brain regions clearly demonstrate the differences

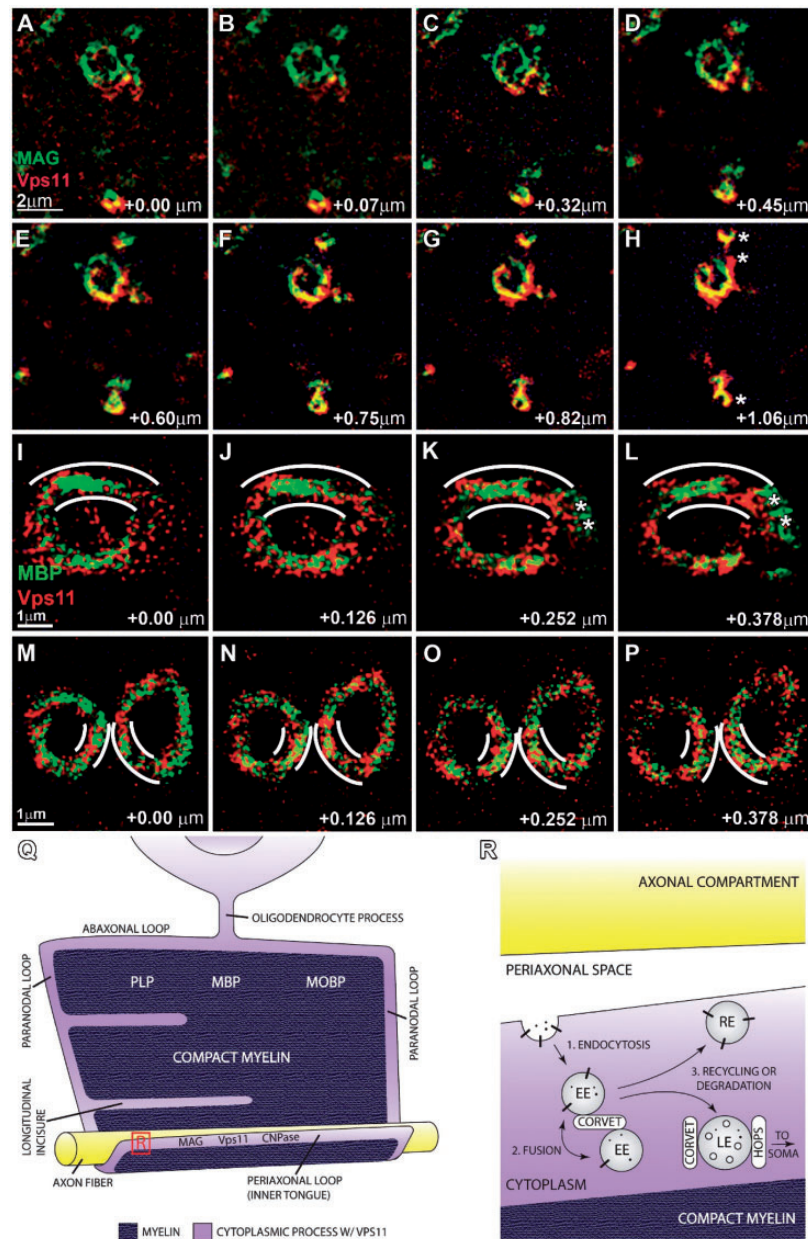


Figure 3. Vps11 Expression Overlaps With MAG Expression in the Inner Tongue of Myelin but Does Not Overlap With MBP in Compact Myelin. A to H: Confocal images from the ventral Basal Ganglia of 15DPN mouse co-immunostained with MAG (green) and Vps11 (red). A and B: Beginning at the top left, MAG surrounds the axon and Vps11 lies in a distinct compartment outside of MAG expression. MAG forms large globules around the axon. C and D: Deeper into the z-plane, MAG and Vps11 begin to co-localize towards the outside of the fiber. E to H: Still deeper into the z-plane, MAG and Vps11 co-localize in the inner tongue of myelin. Transverse cuts of fibers depict the same organization; one of which shows an oligodendrocyte process extending away from the axon, presumably leading back to the cell body, that contains both Vps11 and MAG. I to P: Deconvoluted confocal images from the ventral Basal Ganglia of a 15DPN mouse co-immunostained with MBP (green) and Vps11 (red). Transverse cuts of three different fibers are shown with the relative inner and outer boundaries of myelin highlighted with lines. Note that Vps11 stains both inner and outer loop of myelin but is negligible in compact myelin. Asterisks in K and L likely represent MBP in the cytoplasmic compartment around the paranode/node outside of compact myelin. Q: Schematic illustrating a working model of Vps11 localization in association with other major molecules in myelin. Red box shows inset location for panel R. R: Diagram illustrates a simplified cartoon of the uptake of molecules from plasma membrane of oligodendrocytes, shuttling to early endosomes (EE) where Vps11 is located as a component of CORVET complex. Next, products are either recycled via recycling endosomes (RE) or sent to late endosomes (LE) for shuttling back to the oligodendrocyte soma for degradation. In this case, Vps11 would function as both a component of the CORVET and HOPS complexes.

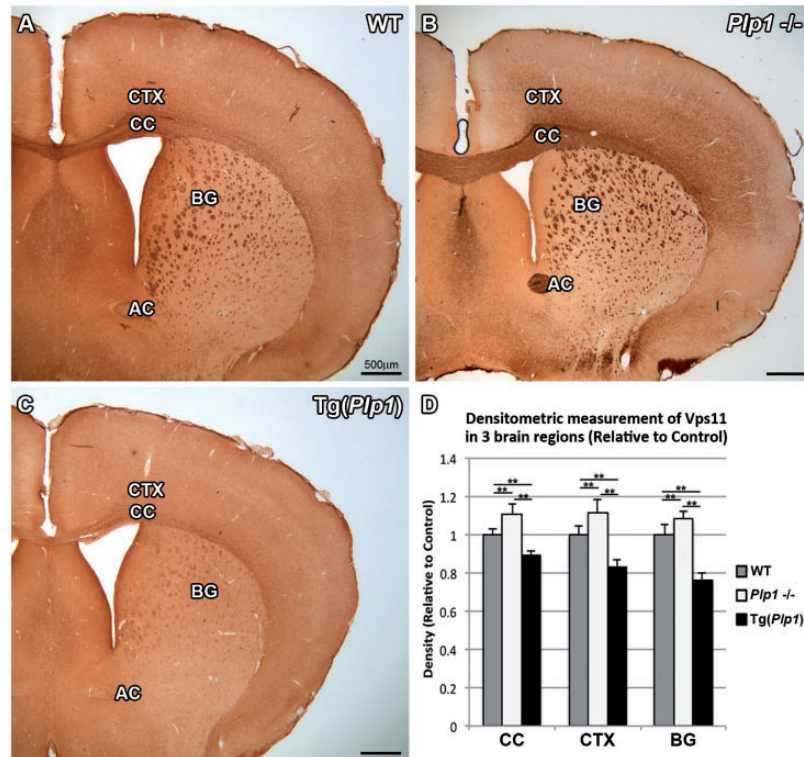


Figure 4. Vps11 Expression Is Altered in *Plp1* Null Mutants and *Plp1* Mice With Duplications at 30 DPN. Transverse sections from adult wild-type B6 mice (A), *Plp1* null mutant mice (*Plp1*^{-/-}; B), and transgenic mice with duplications of the *Plp1* gene abbreviated in Figures as Tg (C) immunostained for Vps11. Compared with wild-type sections (A), Vps11 expression in oligodendrocyte somas and associated myelin tracks was significantly increased in *Plp1* null mutants (B) and significantly decreased in *Plp1* mice with duplications of the *Plp1* gene (C). D: Graphic representation of densitometric intensity quantification of Vps11 immunostaining in the corpus callosum (CC), cortex (CTX), and basal ganglia (BG). Asterisks indicate significant differences between indicated groups ($p < 0.01$) ($n = 3$ mice per group).

observed in Vps11 immunostaining between their genetic backgrounds (Figure 5). Western blot analysis from whole brain hemispheres confirmed the finding that Vps11 expression significantly decreased in *Plp1* mice with duplications (Figure 5J; $p < 0.01$), but the increase in Vps11 expression in *Plp1* null mice did not reach significance (Figure 5J; $p > 0.05$).

Neurofilament Immuno-Colocalization Shows That Vps11 Is Not Localized to Axons

We next compared Vps11 expression to neurofilament immunostaining to determine whether Vps11 is expressed in axons. We co-immunolabeled Vps11 with neurofilament light chain protein (NF-L, MW 68-70), which detects axonal damage (Khalil et al., 2018; Thompson and Mead, 2019) and protein NF200 (MW 200), which detects both phosphorylated and non-phosphorylated NF (Figures 6 and 7). In addition, we compared these relationships in *Plp1* null mutants and *Plp1* mice with duplications.

In wild-type mice at low magnification (Figure 6A and B), NF-L and Vps11 immunostained the length of the axon, and there was little co-localization of the two

proteins. At higher magnification (Figure 6C), NF-L immunostaining alternated with Vps11 immunostaining, which formed short, globular puncta. In confocal, deconvolved cross sections of axons (Figure 6D), NF-L expression was found primarily in the axon cylinder, whereas Vps11 expression was outside of the NF-L-positive axonal compartment. In *Plp1* null mice, we observed that Vps11 immunofluorescence was increased compared to wild-type mice (Figure 6E to H), which agreed with the DAB staining (Figure 4). Similar to wild-type mice, Vps11 expression remained largely outside of the NF-L-positive axonal compartment in both longitudinal and transverse sections of axons (Figure 6E to H). In *Plp1* mice with duplications, Vps11 expression was decreased when compared with wild-type mice; weak expression again localized to globular puncta in longitudinal sections (Figure 6I to K), and expression remained outside of the NF-L-positive compartment in transverse sections (Figure 6L).

Similar to NF-L expression, NF200 immunostaining in wild-type mice co-localized with Vps11 in globular puncta within the Vps11-positive myelin sheath (Figure 7A to C). Unlike NF-L expression, this co-localization was

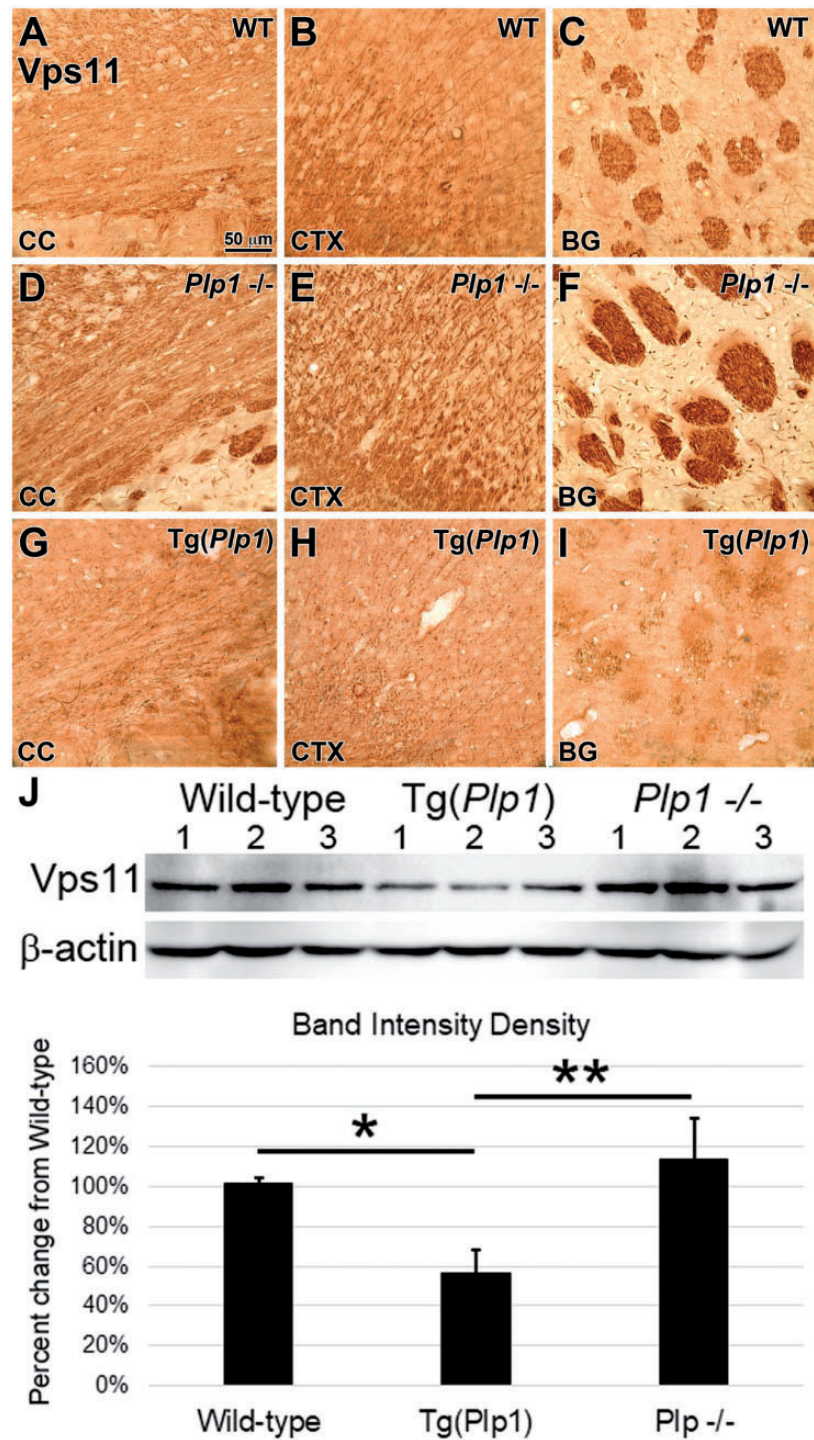


Figure 5. High Magnification Images and Western Blot Analysis of Vps11 Expression in *Plp1* Null Mutants and *Plp1* Mice with Duplications. Representative high magnification images of Vps11 expression from various regions of adult wild-type B6 mice (WT; A to C), *Plp1* null mutant mice (*Plp1*^{-/-}; D to F), and transgenic mice with duplications of the *Plp1* gene (*Tg(Plp1)*; G to I), include the corpus callosum (CC), cortex (CTX), and basal ganglia (BG). Differences in levels of expression between wild-type and transgenic mice are obvious. All sections were processed identically. J: Western blot analysis of Vps11 expression from brain hemispheres of adult wild-type B6 mice (Wild-type), transgenic mice with duplications of the *Plp1* gene (*Tg(Plp1)*), and *Plp1* null mutant mice (*Plp1*^{-/-}) (n = 3 mice per group). Graphical representation of normalized Vps11 band intensity density based on percent change from wild-type. Statistical differences between the groups was determined using a one-way ANOVA followed by a post-hoc Tukey test (*p < 0.05; **p < 0.01).

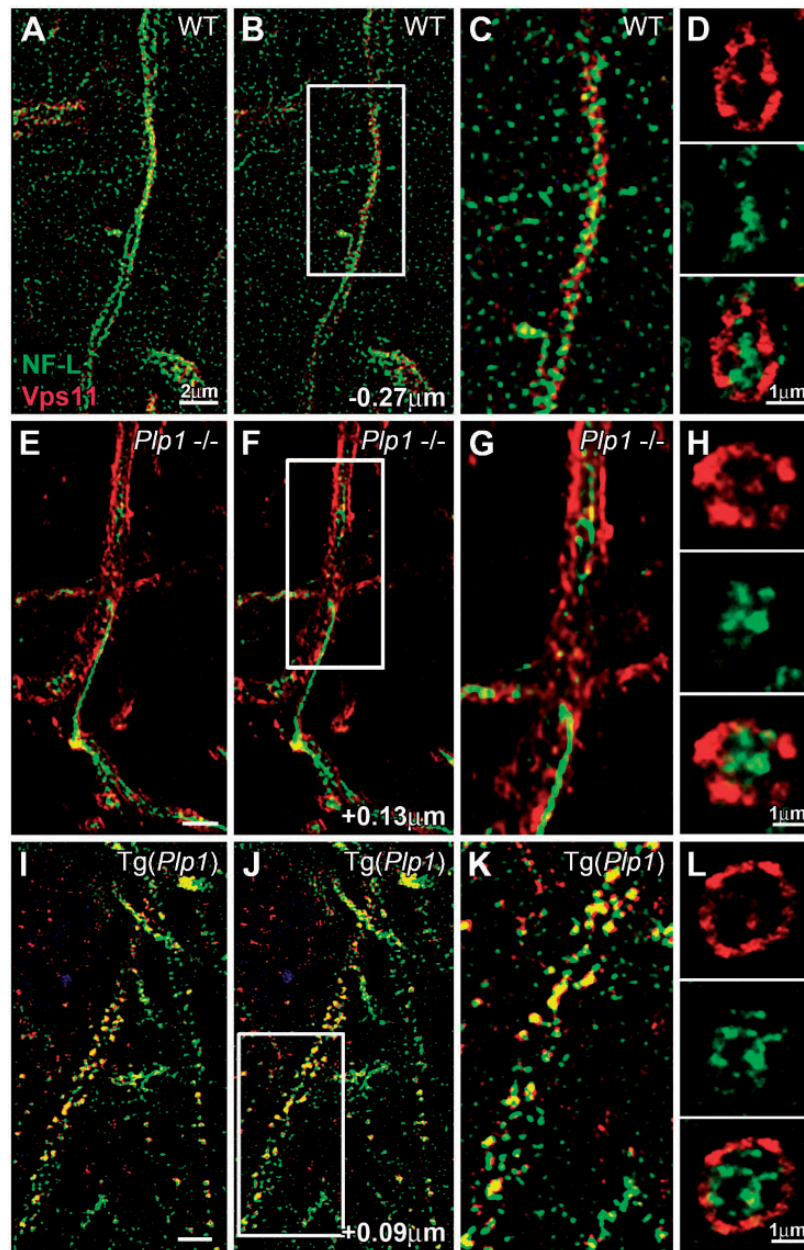


Figure 6. Comparison of NF-L and Vps11 Immunolocalization in Wild-Type, *Plp1* Null Mutants and *Plp1* Mice With Duplications. A to D: Confocal images from the ventral Basal Ganglia of adult wild-type (WT) B6 mice immunostained with NF-L (green) and Vps11 (red). Longitudinal sections through the axon of WT-mice (A to C) show Vps11 expression alternates with NF-L expression. Confocal, deconvolved, cross-sections through the axon (D) confirmed that Vps11 expression was immediately outside of the axon. E-G. Confocal images from 35DPN *Plp1* null mutant mice immunostained with NF-L (green) and Vps11 (red). Longitudinal and cross sections through the axon (E to G) show strong Vps11 expression was largely distinct from NF-L, and in agreement with quantitative Vps11 immunostaining visualized with DAB. H. Confocal deconvolved, cross-sections through the axon confirmed Vps11 expression was immediately outside the axon. I to L. Confocal images from *Plp1* mice with duplications immunostained with NF-L (green) and Vps11 (red). Images suggest degeneration of axon cylinder. Longitudinal sections through the axon (I to K) show very weak Vps11 expression overlapping with a subset of NF-L-positive puncta. Again, cross-sections through the axon (L) confirmed that Vps11 expression was immediately outside of the axon and NF-L staining within the axon proper.

observed even at low magnification (Figure 7A and B). This expression pattern did not change in *Plp1* null mutant mice, despite the overall increase in Vps11 expression (Figure 7E to H). However, in *Plp1* mice with

duplications, Vps11 co-localization of NF200 and Vps11 was frequently observed (Figure 7I to L). Transverse sections of axon fibers confirmed co-localization of NF200 and Vps11 outside the axon in *Plp1* overexpression mice

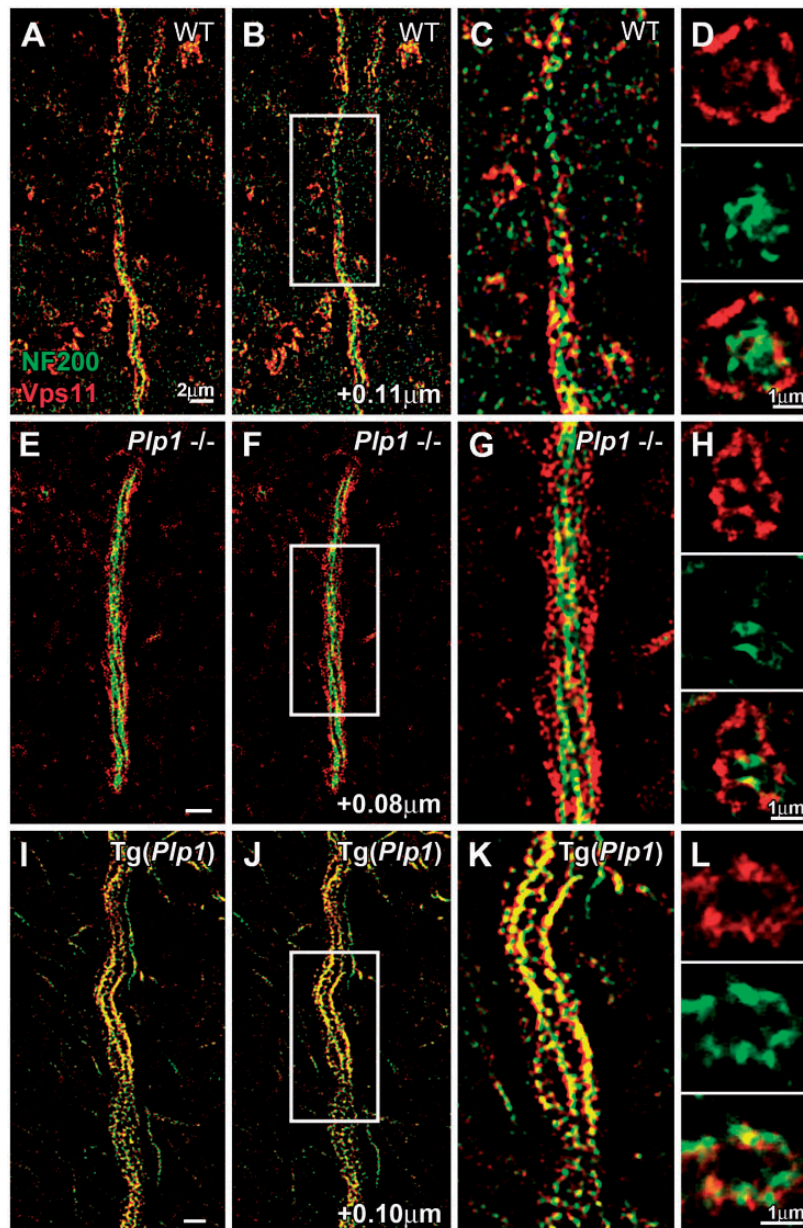


Figure 7. Comparison of NF200 and Vps11 Immunolocalization in Wild-Type, *Plp1* Null Mutants and *Plp1* Mice With Duplications. A to D. Confocal images from the ventral Basal Ganglia of adult WT-B6 mice immunostained with NF200 (green) and Vps11 (red). Longitudinal sections through the axon (A to C) show Vps11 expression was largely distinct from NF200. D: Confocal deconvolved, cross-sections through the axon confirmed that Vps11 expression was immediately outside of the axon. E to H: Confocal images from adult *Plp1* null mutant mice immunostained with NF200 (green) and Vps11 (red). Longitudinal and cross sections through the axon of a mouse with duplications (E to G) show strong Vps11 expression was largely distinct from NF200. H: Confocal, deconvolved cross-sections through the axon confirmed that Vps11 expression was immediately outside the axon. (I to L) Confocal images from adult *Plp1* mutant mice with duplications immunostained with NF200 (green) and Vps11 (red). Longitudinal sections through the axon (I to K) show Vps11 expression overlapping in a subset of NF200-positive puncta. L: Cross-sections through the axon confirmed that Vps11 expression was immediately outside of the axon, but showed weak NF200 staining within the adaxonal membrane.

(Figure 7L), suggesting the presence of axonal breakdown in the mice with duplications. However, at our current resolution, we cannot rule out the possibility that Vps11 is instead up-regulated in the axon in these animals.

In summary, numerous longitudinal and transverse sections of axons showed that Vps11 is not present in the axonal compartment. Consistent with our findings using DAB staining, Vps11 immunofluorescence appears

increased in *Plp1* null mice and decreased in *Plp1* over-expression mice.

Vps11 and *PDGFR α* Co-Localize to Oligodendrocyte Precursor Cells

As *PDGFR α* is an established marker for OPCs (Marques et al., 2016), and should undergo retrograde transport of PDGF back to the cell body, we investigated whether it co-localized with *Vps11*. In cultured oligodendrocyte cells, we observed co-localization of the two molecules in round puncta, suggestive of organelle structures (Figure 8A to F). While this finding does not definitively demonstrate retrograde transport of PDGF back to the

cell body, co-localization of *Vps11* and *PDGFR α* within round organelles strongly suggests they reside within the endolysosomal system. *In vivo*, co-localization of the two antibodies (Figure 8G to L) is frequently present in OPCs, many of which are in or immediately adjacent to the subventricular zone.

Vps11 Co-Localizes With Established Markers of the Endolysosomal System

To confirm that our antisera for *Vps11* localized to proteins of the endolysosomal system in oligodendrocytes, we co-labeled *Vps11* with EEA1 (Figure 9A to F) and *Lamp2* (Figure 9G to L), an established marker for late

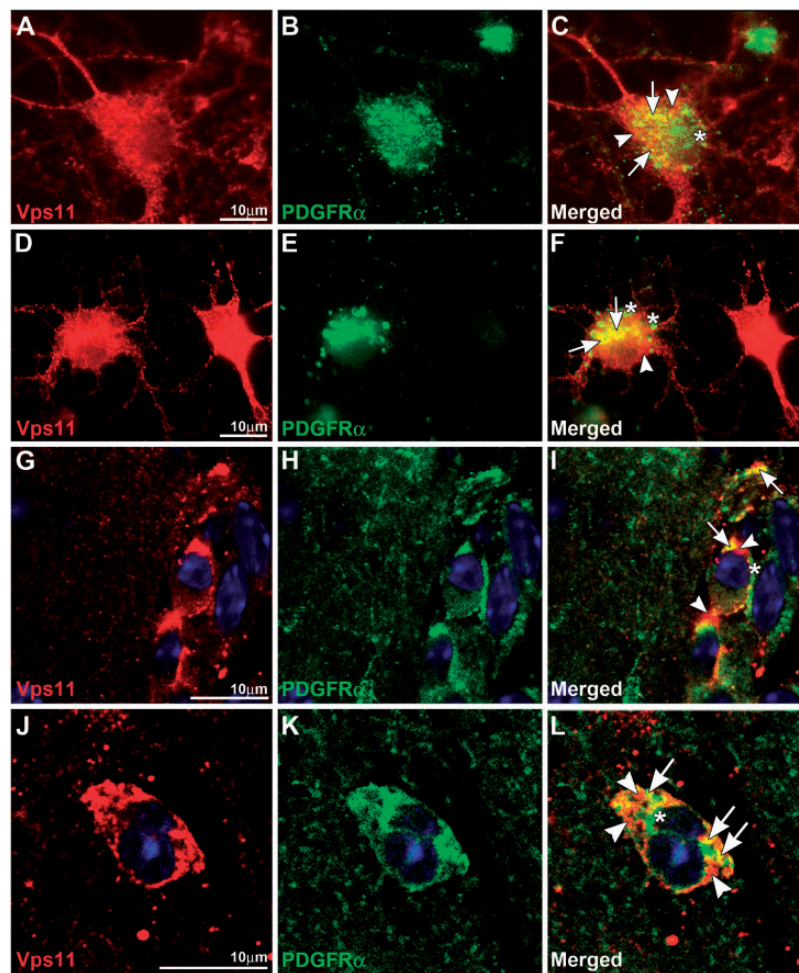


Figure 8. Combined immunofluorescent Staining With *PDGFR α* and *Vps11* of Enriched 7-Day Old Oligodendrocyte Cultures and 15DPN Mouse Brains. A to F: *PDGFR α* and *Vps11* immunostaining of enriched 7 day old oligodendrocyte culture. A and D: *Vps11* is present throughout perikarya and processes of OPCs. B and E: *PDGFR α* is present mainly in perikarya but extends into proximal processes. C and F: Co-localization of the 2 antibodies (arrows) in round organelles is abundant, but organelles where *PDGFR α* is separate from *Vps11*, and vice-versa, is noticeable in both OPCs (arrowheads and asterisks). Note the cell to the right in panel F is *Vps11*+ and *PDGFR α* -, indicating specificity of antibody. G to L: *PDGFR α* and *Vps11* immunostaining of cells from the ventral Basal Ganglia of a 15DPN mouse brain shows spotty co-localization in perikarya. These cells are likely oligodendrocytes due to the strong expression of *Vps11*. In addition, we have previously described *PLP*+ and *MOG*+ OPCs in this region (Jalabi et al., 2003). Arrows point to co-localization of the two antibodies, whereas arrowheads and asterisk point to distinct expression of each antibody.

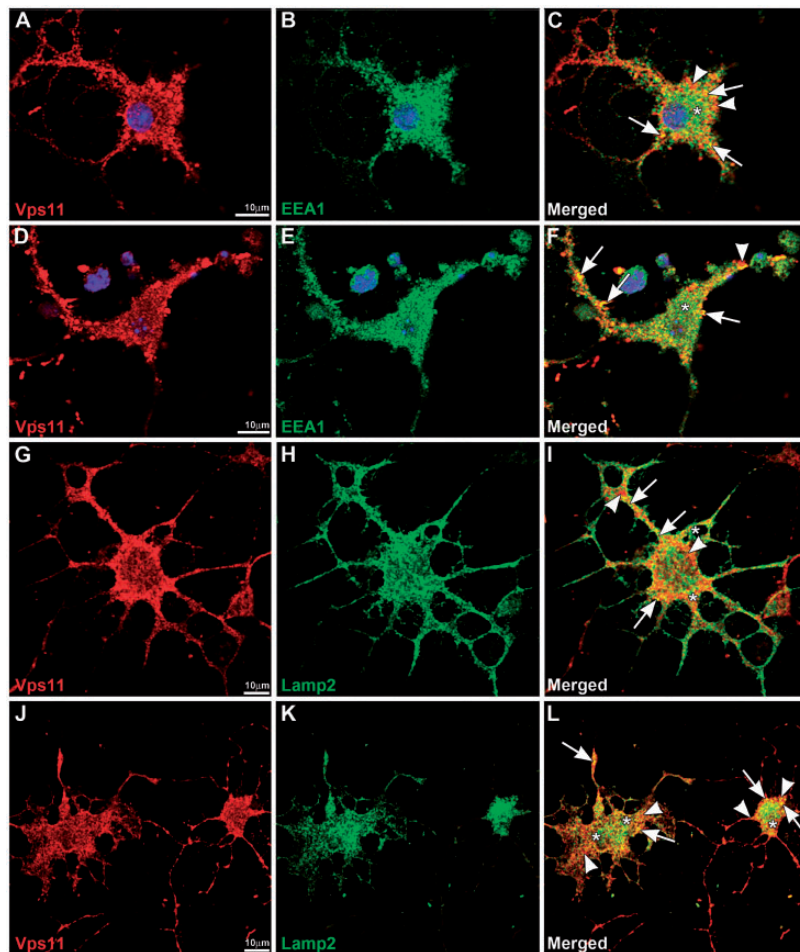


Figure 9. Combined Immunofluorescent Staining With EEA1, Lamp2 and Vps11 Antibodies of Enriched 7-Day Old Oligodendrocyte Cultures. A to F: EEA1 (green) and Vps11 (red) immunostaining of enriched 7 day old oligodendrocyte culture. Arrows point to co-localization of the two antibodies. Arrowheads point to Vps11 expression distinct from EEA1 expression and asterisks point to EEA1 expression distinct from Vps11. G-L. Lamp2 (green) and Vps11 (red) immunostaining of enriched 7 day old oligodendrocyte culture. Arrows point to co-localization of the two antibodies. Arrowheads point to Vps11 expression distinct from Lamp2 expression and asterisks point to Lamp2 expression distinct from Vps11.

endosomes/lysosomes (Fraser et al., 2019). *In vitro*, we observed that Vps11 extensively co-localized to both EEA1 and Lamp2-positive puncta, which is consistent with a conserved role of C-Vps proteins to accommodate the fusion of late endosomes to lysosomes (Balderhaar and Ungermann, 2013; van der Kant et al., 2015). Collectively, our data indicate that Vps11, a well-established and conserved component of the endolysosomal system, is found within oligodendrocyte cytoplasm that extends to the inner tongue of myelin.

Discussion

Vps11 is one of many proteins involved in the fusion of endosomal organelles and in the transport of molecules from endosomal compartments to lysosomes for degradation. As noted in the Introduction, our knowledge of

the localization and function of the CORVET and HOPS complexes is mainly derived from studies of yeast (Rossi et al., 1990; Peplowska et al., 2007; Markgraf et al., 2009; Balderhaar and Ungermann, 2013; van der Kant et al., 2015; Takemoto et al., 2018). However, a limited number of studies in vertebrates including zebrafish, catfish, dogs, mice and humans have documented the highly conserved nature of the CORVET and HOPS complexes (Jiang et al., 2014; Perini et al., 2014; McEwan et al., 2015; Wartosch et al., 2015). In the vertebrate brain, the *VPS11* gene has been identified as a biomarker in Parkinson's disease (Jiang et al., 2014). A missense mutation in *Vps11* has been identified in Rottweiler dog brains with neuroaxonal dystrophy (He et al., 2018; Lucot et al., 2018). Most significantly, hypomyelination in Ashkenazi-Jewish patients is associated with a founder effect mutation in *VPS11* (Edvardson et al., 2015; Zhang et al.,

2016), and this same mutation inhibits morphological differentiation in the mouse oligodendroglial FBD-102 cell line (Matsumoto et al., 2020). These few mammalian studies highlight the importance of endolysosomal trafficking in normal brain function and myelin integrity. However, the neural cell types expressing Vps11 in mammals have not been identified.

Herein we provide evidence for strong expression of Vps11 protein in oligodendrocytes, and its unique localization at the axon-myelin interface. Vps11 should be ubiquitously expressed in all cell types with endolysosomal trafficking, and a previous single-cell RNAseq database suggests a relative equal distribution of *Vps11* mRNA within cells from the mouse cortex (Zeisel et al., 2015). We do not dispute these findings, but note that mRNA expression does not always equate to protein expression. Using both double immunofluorescence and DAB immunostaining, we did not detect strong Vps11 expression in other cell types of the brain *in vivo*. However, we cannot eliminate the possibility (indeed, likelihood), of low levels of Vps11 in other cell types.

In vivo, Vps11 localizes to cells in the white matter with the classical morphology of OPCs/oligodendrocytes (Figure 1). These cells are round or oval, smoothly contoured with several, fine processes emanating from modestly-sized perikarya. They are uniquely different from astrocytic and microglial morphology. Definitive identification of oligodendrocytes as bearers of Vps11 comes from double-labeling studies with Vps11 and MBP (Figure 2). Generally, the two proteins are in separate compartments; predictably so, as MBP mRNA is transported mainly on free ribosomes to incipient myelin sheaths where it is translated (Muller et al., 2013). However, during development, when MBP message and protein levels are high, MBP can be visualized in the oligodendrocyte perikarya (Sternberger et al., 1978). Consistent with this result, our initial studies failed to find co-localization of MBP and Vps11 in oligodendrocyte perikarya in mice 1 month and older. *In vitro*, Vps11 was detectable in late-stage OPCs as well as in mature oligodendrocytes but appeared more abundant in OPCs (Figure 1). *In vitro*, localization of Vps11 was similar to that of PLP but there was not complete overlap. Vps11 was mainly present in the vein-like, cytoplasmic channels along with PLP, whereas PLP was also present in their sheets, thought to be unfurled compact myelin. *In vitro*, cells with flattened, sheet-like cytoplasm and/or straight and thick processes (i.e. astrocytic morphology) were Vps11 and GFAP positive (Figure 1G to I). Thus, Vps11 cellular distribution *in vitro* is likely different from *in vivo*.

In vivo, low magnification pictures of Vps11 show strong staining in myelin; however, at higher magnification, it is not in compact myelin, but is similar to MAG. Co-localization of Vps11 and MBP shows MBP stains

the length of the myelin sheath whereas Vps11 forms bead-like structures that are very noticeable in longitudinal and transverse sections of myelin (Figure 2). Along the length of the axon, Vps11 is clearly observed in a separate compartment than MBP, presumably in the oligodendrocyte cytoplasm forming paranodal loops, periaxonal (inner tongue) and abaxonal (outer tongue) compartments (Figures 2 and 3). In support of this, co-immunostaining of Vps11 and MBP in transverse sections of fibers confirmed that Vps11 stains both inner and outer loops of myelin but is negligible in compact myelin (Figure 3I to P). Double immunofluorescence with MAG and VPS11 predictably shows MAG in the periaxonal (inner tongue) process immediately adjacent to axonal plasma membrane and is clearly not found in axoplasm of wild-type mice. Focusing through the z-plane of deconvolved confocal images, Vps11 approaches the inner tongue from oligodendrocyte processes separate from MAG but then the expression of the two proteins overlaps nearly completely in forming a circumferential pattern around an axon (Figure 3).

Collectively, these co-immunolocalization studies suggest that the endolysosomal system involving the C-Vps proteins extends to the compartment immediately adjacent to the axon. However, a word of caution here regarding apparent “co-localization.” The interpretation that co-localization of two proteins are in the same compartment should be judicious given that the double-labeling may simply reflect overlap of the two fluorescent colors stacked on top of each other in the confocal images. Even with confocal imaging, the thickness of the captured image is approximately 0.25 μm using the Leica TCS SP8. Since plasma membranes are $\sim 7.5\text{--}10\text{ nm}$ (0.075–0.01 μm), an apparent overlap between a myelin plasma membrane and adjacent cytoplasm is possible. Therefore, the overlap of MAG and Vps11 in the inner tongue with confocal microscopy does not confirm co-localization of MAG to Vps11-positive endosomes, but only provides the first line of evidence that Vps11 is present with MAG in the periaxonal compartment.

Evidence that Vps11 is not present (or present at non-detectable low levels) in axons is observed by co-immunostaining of Vps11 with antibodies to two neurofilament proteins (NF-L (MW68-70) and Neurofilament 200 (MW200)). In both longitudinal and transverse sections through axons (Figures 6 and 7), Vps11 often presents as a bead-like appearance much like that seen with combined Vps11 and MBP. Combined immunofluorescence with Vps11 and low or high neurofilament antibodies confirms the absence of Vps11 in the axonal compartment (Figures 6 and 7). The intensity of Vps11 immunostaining in the *Plp1* mice with duplications shows an apparent Vps11 decrease in these mice, similar to that seen with Vps11 DAB immunostaining (Figures 4 and 5). This observation is

consistent with our observation of abundant axonal degeneration in these mice at 1 month, whereas in the *Plp1*-null mice axonal degeneration is hardly detectable at this age (*data not shown*). Modest alterations of fast anterograde and retrograde axoplasmic transport have been detected in *Plp1* null mice beginning at 1-2 months (Edgar et al., 2004). Immunoblotting of NF-L and NF200 at 2 months did not reveal differences between *Plp1*-nulls and wild-type mice (Edgar et al., 2004). However, it is possible that these preparations did not contain the inner tongue processes of oligodendrocytes or levels of degradation are very low. Therefore, based upon present data sets, it is difficult to conclude whether increased degradation of neurofilaments in oligodendrocyte cytoplasm occurs. Extensive additional biochemical and quantitative experiments need to be performed to detect turnover of neurofilaments in oligodendrocyte processes.

As evidenced by comparing levels of Vps11 in mice with *Plp1* duplications and deletions, we found a significant correlation of expression of Vps11 protein levels to that of PLP. At one month, Vps11 immunolocalization is significantly increased in *Plp1* null mice by 15% and significantly decreased in *Plp1* mice with duplications by 25% (Figure 4D). Western blot analysis confirmed the finding that Vps11 expression significantly decreased in *Plp1* mice with duplications (Figure 5J; $p < 0.01$), but the increase in Vps11 expression in *Plp1* null mice did not reach significance (Figure 5J; $p > 0.05$). The Vps11 increase in the *Plp1* null mice may involve uptake of degenerated products or may simply reflect up-regulation of Vps11 linked to various cellular processes. This latter possibility is likely, as there are many changes to myelin resulting from developmental changes in PLP expression level. Indeed, as neither the *Plp1*-null mice nor the *Plp1* mice with duplications are conditional, alterations in Vps11 expression may result from other genetic and/or biological changes. Therefore, these findings do not demonstrate that PLP controls Vps11 expression, but rather that changes to Vps11 expression are associated with PLP-dependent alterations in myelin.

To understand whether Vps11 functions as a retrograde transporter of molecules from axon to cell body, we examined PDGFR α as it is a well-documented receptor on OPCs/oligodendrocytes (Đăng et al., 2019), presumably regulating OPC proliferation via its agonist PDGF. While we did not grow cells with PDGF, colocalization of Vps11 and PDGFR α was present in OPCs. The receptor and Vps11 was abundant in round vesicles, suggestive of its involvement in retrograde transport. Vps11 and PDGFR α were also found in separate compartments, not only indicating specificity of antibody staining, but also predictive of their localization in transport to/from oligodendrocyte/axon interface. It is important to consider, co-localization in the inner tongue does not mean that Vps11 directly binds proteins at the axon-myelin interface. Rather, based on the function of Vps11

in other systems, we predict that it functions in the inner tongue as part of the COVET/HOPS complexes where it is involved in trafficking from early endosomes to lysosomes (see model in Figure 3R).

Surprisingly, virtually nothing is known about proteins involved in uptake at axon-myelin interface and transfer to the CORVET/HOPS complexes. This study potentially opens a new area of research, with highlighted importance due to the recent finding of a *VPS11* mutation in humans. The early literature on oligodendrocyte interactions dates back to the early 1980's when George Allt in 1982 (Allt and Ghabriel, 1982) hypothesized that there must be crosstalk between the two cell types. The authors noted at the time that "crosstalk between axon and the two cell types (Schwann cell and oligodendrocyte) can be interrupted and hence demyelination initiated..." (Allt and Ghabriel, 1982). Recent studies involving gain or loss of function of myelin proteins usually combined with axonal degeneration, clearly demonstrate reciprocal interactions between oligodendrocytes and axons. Myelin breakdown products must be degraded around the myelin sheath, astrocytes and microglia (Wang et al., 2020) or, more likely, transported back to the oligodendrocyte cell body for degradation by established organelles such as lysosomes and proteasomes. The literature is rife with reports of axon glial interactions but scant about molecules involved in myelin-axon communication (Nave and Trapp, 2008; Reiter and Bongarzone, 2020; Wang et al., 2020). Particularly important to this field may be findings related to lysosomal brain disorders (Fraldi et al., 2016; Kett and Dauer, 2016; Kao et al., 2017; Yellajoshiyula et al., 2017) as CORVET/HOPS proteins track to lysosomes in the endolysosomal system. Upstream of lysosomes, virtually nothing is known about aberrations of proteins fused to CORVET/HOPS complexes, let alone proteins of these two complexes. The identification of mutations in *VPS11* that are concomitant with hypomyelination, along with Vps11 localization at the axon-myelin interface, should open new avenues of research into axon-myelin communication and the influence of the endolysosomal system on myelin integrity. Furthermore, given that *VPS11* does not function independently of the other core C-Vps proteins, these findings highlight the need to explore the functional consequences of mutations to the larger group of CORVET/HOPS proteins in oligodendrocytes.

Declaration of Conflicting Interests

The author(s) declared no potential conflicts of interest with respect to the research, authorship, and/or publication of this article.

Funding

The author(s) disclosed receipt of the following financial support for the research, authorship, and/or publication of this article: This work was supported by National Eye Institute

(P30EY04068 and R01EY026551) and Research to Prevent Blindness (Unrestricted Grant).

ORCID iD

Ryan Thummel  <https://orcid.org/0000-0002-0522-8704>

References

- Allt, G., & Ghabriel, M. N. (1982). Demyelination: A failure of cell communication? *Journal of the Neurological Sciences*, *57*(2–3), 287–290.
- Appikarla, S., Bessert, D., Lee, I., Huttemann, M., Mullins, C., Somayajulu-Nitu, M., Yao, F., & Skoff, R. P. (2014). Insertion of proteolipid protein into oligodendrocyte mitochondria regulates extracellular pH and adenosine triphosphate. *Glia*, *62*(3), 356–373.
- Balderhaar, H. J., & Ungermann, C. (2013). CORVET and HOPS tethering complexes—coordinators of endosome and lysosome fusion. *Journal of Cell Science*, *126*(Pt 6), 1307–1316.
- Banta, L. M., Robinson, J. S., Klionsky, D. J., & Emr, S. D. (1988). Organelle assembly in yeast: characterization of yeast mutants defective in vacuolar biogenesis and protein sorting. *The Journal of Cell Biology*, *107*(4), 1369–1383.
- Christoforidis, S., McBride, H. M., Burgoyne, R. D., & Zerial, M. (1999). The Rab5 effector EEA1 is a core component of endosome docking. *Nature*, *397*(6720), 621–625.
- Đäng, T. C., Ishii, Y., Nguyen, V. D., Yamamoto, S., Hamashima, T., Okuno, N., Nguyen, Q. L., Sang, Y., Ohkawa, N., Saitoh, Y., Shehata, M., Takakura, N., Fujimori, T., Inokuchi, K., Mori, H., Andrae, J., Betsholtz, C., & Sasahara, M. (2019). Powerful homeostatic control of oligodendroglial lineage by PDGFR α in adult brain. *Cell Reports*, *27*(4), 1073.e1075–1089.e1075.
- Edgar, J. M., McLaughlin, M., Yool, D., Zhang, S. C., Fowler, J. H., Montague, P., Barrie, J. A., McCulloch, M. C., Duncan, I. D., Garbern, J., Nave, K. A., & Griffiths, I. R. (2004). Oligodendroglial modulation of fast axonal transport in a mouse model of hereditary spastic paraplegia. *The Journal of Cell Biology*, *166*(1), 121–131.
- Edvardson, S., Gerhard, F., Jalas, C., Lachmann, J., Golan, D., Saada, A., Shaag, A., Ungermann, C., & Elpeleg, O. (2015). Hypomyelination and developmental delay associated with VPS11 mutation in Ashkenazi-Jewish patients. *Journal of Medical Genetics*, *52*(11), 749–753.
- Fraldi, A., Klein, A. D., Medina, D. L., & Settembre, C. (2016). Brain disorders due to lysosomal dysfunction. *Annual Review of Neuroscience*, *39*, 277–295.
- Fraser, J., Simpson, J., Fontana, R., Kishi-Itakura, C., Ktistakis, N. T., & Gammoh, N. (2019). Targeting of early endosomes by autophagy facilitates EGFR recycling and signalling. *EMBO Reports*, *20*(10), e47734.
- He, Q., Cui, X., Shen, D., Chen, Y., Jiang, Z., Lv, R., Eremin, S. A., & Zhao, S. (2018). Development of a simple, rapid and high-throughput fluorescence polarization immunoassay for glycocholic acid in human urine. *Journal of Pharmaceutical and Biomedical Analysis*, *158*, 431–437.
- Jalabi, W., Cerghet, M., Skoff, R. P., & Ghandour, M. S. (2003). Detection of oligodendrocytes in tissue sections using PCR synthesis of digoxigenin-labeled probes. *The Journal of Histochemistry and Cytochemistry: Official Journal of the Histochemistry Society*, *51*(7), 913–919.
- Jiang, P., Nishimura, T., Sakamaki, Y., Itakura, E., Hatta, T., Natsume, T., & Mizushima, N. (2014). The HOPS complex mediates autophagosome-lysosome fusion through interaction with syntaxin 17. *Molecular Biology of the Cell*, *25*(8), 1327–1337.
- Kao, A. W., McKay, A., Singh, P. P., Brunet, A., & Huang, E. J. (2017). Progranulin, lysosomal regulation and neurodegenerative disease. *Nature Reviews. Neuroscience*, *18*(6), 325–333.
- Kett, L. R., & Dauer, W. T. (2016). Endolysosomal dysfunction in Parkinson's disease: Recent developments and future challenges. *Movement Disorders: Official Journal of the Movement Disorder Society*, *31*(10), 1433–1443.
- Khalil, M., Teunissen, C. E., Otto, M., Piehl, F., Sormani, M. P., Gattringer, T., Barro, C., Kappos, L., Comabella, M., Fazekas, F., Petzold, A., Blennow, K., Zetterberg, H., & Kuhle, J. (2018). Neurofilaments as biomarkers in neurological disorders. *Nature Reviews. Neurology*, *14*(10), 577–589.
- Klugmann, M., Schwab, M. H., Puhlhofer, A., Schneider, A., Zimmermann, F., Griffiths, I. R., & Nave, K. A. (1997). Assembly of CNS myelin in the absence of proteolipid protein. *Neuron*, *18*(1), 59–70.
- Knapp, P. E., Bartlett, W. P., & Skoff, R. P. (1987). Cultured oligodendrocytes mimic in vivo phenotypic characteristics: Cell shape, expression of myelin-specific antigens, and membrane production. *Developmental Biology*, *120*(2), 356–365.
- Lucot, K. L., Dickinson, P. J., Finno, C. J., Mansour, T. A., Letko, A., Minor, K. M., Mickelson, J. R., Drögemüller, C., Brown, C. T., & Bannasch, D. L. (2018). A missense mutation in the vacuolar protein sorting 11 (*VPS11*) gene is associated with neuroaxonal dystrophy in rottweiler dogs. *G3 (Bethesda)*, *8*, 2773–2780.
- Markgraf, D. F., Ahnert, F., Arlt, H., Mari, M., Peplowska, K., Epp, N., Griffith, J., Reggiori, F., & Ungermann, C. (2009). The CORVET subunit Vps8 cooperates with the Rab5 homolog Vps21 to induce clustering of late endosomal compartments. *Molecular Biology of the Cell*, *20*(24), 5276–5289.
- Marques, S., et al. (2016). Oligodendrocyte heterogeneity in the mouse juvenile and adult central nervous system. *Science (New York, N.Y.)*, *352*(6291), 1326–1329.
- Matsumoto, N., Miyamoto, Y., Hattori, K., Ito, A., Harada, H., Oizumi, H., Ohbuchi, K., Mizoguchi, K., & Yamauchi, J. (2020). PP1C and PP2A are p70S6K phosphatases whose inhibition ameliorates HLD12-associated inhibition of oligodendroglial cell morphological differentiation. *Biomedicine*, *8*(4), 89.
- McEwan, D. G., Popovic, D., Gubas, A., Terawaki, S., Suzuki, H., Stadel, D., Coxon, F. P., Miranda de Stegmann, D., Bhogaraju, S., Maddi, K., Kirchof, A., Gatti, E., Helfrich, M. H., Wakatsuki, S., Behrends, C., Pierre, P., & Dikic, I. (2015). PLEKHM1 regulates autophagosome-lysosome fusion through HOPS complex and LC3/GABARAP proteins. *Molecular Cell*, *57*(1), 39–54.

- Muller, C., Bauer, N. M., Schafer, I., & White, R. (2013). Making myelin basic protein -from mRNA transport to localized translation. *Frontiers in Cellular Neuroscience*, 7, 169.
- Nave, K. A., & Trapp, B. D. (2008). Axon-glia signaling and the glial support of axon function. *Annual Review of Neuroscience*, 31, 535–561.
- Nickerson, D. P., Brett, C. L., & Merz, A. J. (2009). Vps-C complexes: Gatekeepers of endolysosomal traffic. *Current Opinion in Cell Biology*, 21(4), 543–551.
- Nielsen, E., Christoforidis, S., Uttenweiler-Joseph, S., Miaczynska, M., Dewitte, F., Wilm, M., Hoflack, B., & Zerial, M. (2000). Rabenosyn-5, a novel Rab5 effector, is complexed with hVPS45 and recruited to endosomes through a FYVE finger domain. *The Journal of Cell Biology*, 151(3), 601–612.
- Peplowska, K., Markgraf, D. F., Ostrowicz, C. W., Bange, G., & Ungerer, C. (2007). The CORVET tethering complex interacts with the yeast Rab5 homolog Vps21 and is involved in endo-lysosomal biogenesis. *Developmental Cell*, 12(5), 739–750.
- Perini, E. D., Schaefer, R., Stoter, M., Kalaidzidis, Y., & Zerial, M. (2014). Mammalian CORVET is required for fusion and conversion of distinct early endosome subpopulations. *Traffic (Copenhagen, Denmark)*, 15(12), 1366–1389.
- Raymond, C. K., Howald-Stevenson, I., Vater, C. A., & Stevens, T. H. (1992). Morphological classification of the yeast vacuolar protein sorting mutants: Evidence for a pre-vacuolar compartment in class E vps mutants. *Molecular Biology of the Cell*, 3(12), 1389–1402.
- Readhead, C., Schneider, A., Griffiths, I., & Nave, K. A. (1994). Premature arrest of myelin formation in transgenic mice with increased proteolipid protein gene dosage. *Neuron*, 12(3), 583–595.
- Reiter, C. R., & Bongarzone, E. R. (2020). The role of vesicle trafficking and release in oligodendrocyte biology. *Neurochemical Research*, 45(3), 620–629.
- Rossi, A., De Cataldo, S., Di Michele, V., Manna, V., Ceccoli, S., Stratta, P., & Casacchia, M. (1990). Neurological soft signs in schizophrenia. *The British Journal of Psychiatry: The Journal of Mental Science*, 157, 735–739.
- Spang, A. (2016). Membrane tethering complexes in the endosomal system. *Frontiers in Cell and Developmental Biology*, 4, 35.
- Sternberger, N. H., Itoyama, Y., Kies, M. W., & Webster Hd, (1978). Immunocytochemical method to identify basic protein in myelin-forming oligodendrocytes of newborn rat C. N.S. *J Neurocytol*, 7, 251–263.
- Sternberger, N. H., Quarles, R. H., Itoyama, Y., & Webster, H. D. (1979). Myelin-associated glycoprotein demonstrated immunocytochemically in myelin and myelin-forming cells of developing rat. *Proceedings of the National Academy of Sciences of the United States of America*, 76(3), 1510–1514.
- Takemoto, K., Ebine, K., Askani, J. C., Kruger, F., Gonzalez, Z. A., Ito, E., Goh, T., Schumacher, K., Nakano, A., & Ueda, T. (2018). Distinct sets of tethering complexes, SNARE complexes, and rab GTPases mediate membrane fusion at the vacuole in arabidopsis. *Proceedings of the National Academy of Sciences of the United States of America*, 115(10), E2457–E2466.
- Tall, G. G., Hama, H., DeWald, D. B., & Horazdovsky, B. F. (1999). The phosphatidylinositol 3-phosphate binding protein Vac1p interacts with a rab GTPase and a Sec1p homologue to facilitate vesicle-mediated vacuolar protein sorting. *Molecular Biology of the Cell*, 10(6), 1873–1889.
- Thompson, A. G. B., & Mead, S. H. (2019). Review: Fluid biomarkers in the human prion diseases. *Molecular and Cellular Neurosciences*, 97, 81–92.
- van der Kant, R., Jonker, C. T., Wijdeven, R. H., Bakker, J., Janssen, L., Klumperman, J., & Neeffjes, J. (2015). Characterization of the mammalian CORVET and HOPS complexes and their modular restructuring for endosome specificity. *The Journal of Biological Chemistry*, 290(51), 30280–30290.
- Wang, F., Ren, S. Y., Chen, J. F., Liu, K., Li, R. X., Li, Z. F., Hu, B., Niu, J. Q., Xiao, L., Chan, J. R., & Mei, F. (2020). Myelin degeneration and diminished myelin renewal contribute to age-related deficits in memory. *Nature Neuroscience*, 23(4), 481–486.
- Wartosch, L., Gunesdogan, U., Graham, S. C., & Luzio, J. P. (2015). Recruitment of VPS33A to HOPS by VPS16 is required for lysosome fusion with endosomes and autophagosomes. *Traffic (Copenhagen, Denmark)*, 16(7), 727–742.
- Yellajoshiyula, D., Liang, C. C., Pappas, S. S., Penati, S., Yang, A., Mecano, R., Kumaran, R., Jou, S., Cookson, M. R., & Dauer, W. T. (2017). The DYT6 dystonia protein THAP1 regulates myelination within the oligodendrocyte lineage. *Developmental Cell*, 42(1), 52.e54–67.e54.
- Zeisel, A., Muñoz-Manchado, A. B., Codeluppi, S., Lönnerberg, P., La Manno, G., Juréus, A., Marques, S., Munguba, H., He, L., Betsholtz, C., Rolny, C., Castelo-Branco, G., Hjerling-Leffler, J., & Linnarsson, S. (2015). Cell types in the mouse cortex and hippocampus revealed by single-cell RNA-seq. *Science*, 347(6226), 1138–1142.
- Zhang, J., et al. (2016). A founder mutation in VPS11 causes an autosomal recessive leukoencephalopathy linked to autophagic defects. *PLoS Genetics*, 12(4), e1005848.